

Structural and Topological Characterization of the Three-Electron Bond: The SO Radicals

Isabelle Fourré^{*,†} and Jacqueline Bergès^{†,‡}

Laboratoire de Chimie Théorique, Université Pierre et Marie Curie, UMR-CNRS 7616, 4 place Jussieu, 75252 Paris Cedex 05, France, and Université René Descartes, Paris Cedex 06, France

Received: July 25, 2003; In Final Form: October 16, 2003

Although a two-center three-electron (2c-3e) bond between homonuclear atoms is well characterized, this is not the case for the S:O bond, especially in neutral radicals resulting from the addition of a hydroxyl group on various sulfur substrates. A structural, energetical, and topological study is presented for prototypical radicals, ionic and neutral, RSOH⁻, RR'SOH₂⁺, and RR'SOH, with R, R' = H, CH₃. Three calculation methods have been applied, BH&HLYP, MP2, and CCSD(T), with different basis sets to determine the domains of accuracy of the more approximate ones to use them for larger systems. Qualitative and quantitative criteria, defined from the topological analysis of the electron localization function, are proposed to characterize such a 2c-3e bond. They specify the number and type of basins and their hierarchy of bifurcation, the global charge transfer between the fragments, the localization of the integrated spin density, and the electron delocalization between the lone pairs of the interacting atoms. Surprisingly, the neutral radicals show an intermediate behavior between the pure 2c-3e S:O bond in anions and the electrostatic interaction in cations, despite the low energy of bond formation. As in the radical anions, the substitution favors the formation of a 2c-3e bond.

I. Introduction

After irradiation of biological systems by high-energy radiation, many sulfur-centered radicals are obtained, resulting from the action of solvated electrons or hydroxyl radicals as products of the decomposition of water. Among these radicals, many three-electron-bonded systems are observed, especially in ionic forms (anions and cations), but several are neutral (for more details, see refs 1–5 and references therein). These radicals are short-living species so they are not easy to characterize as well experimentally as theoretically. Therefore we have to rely on simpler molecular models, for instance, oxidation of dimethyl sulfide (DMS) in aqueous solution for the reactions of hydroxyl radicals formed in body tissue.⁵

Indeed the reaction of dimethyl sulfide (DMS) with hydroxyl radical has been the subject of many experimental and theoretical investigations. It is of crucial importance for oxidations of organic sulfides in the gas phase and in solution, refs 1, 5–10 and references therein. A number of kinetic studies have been carried out and lead to the assumption that the first step of the oxidation consists of competitive attacks of OH at the carbon and sulfur atoms. So the two initial pathways are the addition of OH to the sulfur atom to form the sulfuranyl radical DMSOH and the abstraction of a hydrogen from a carbon atom by the hydroxyl radical. The H-abstraction channel can occur after (or in competition with) the formation of the addition complex DMSOH, which was first proposed by Hynes et al. in their kinetic studies.^{6,11} For instance, stable adducts R₂SOH can be formed by pulse radiolysis of an aqueous solution and their transient formation can be pointed out by the observation of a UV absorption band around 340 nm.⁵ The question of the stability of the adduct and its dissociation energetics is of critical

importance for understanding the mechanism of the DMS oxidation in the gas phase and in solution.

The purpose of the present work is not to study the two pathways but first to discuss the presence or absence of a stable adduct and second to have an insight on the nature of S–O-bonded sulfuranyl radicals. This has been the subject of several previous investigations,^{8,12,13} but until now, there is no agreement between the results of ab initio calculations^{7,9,10} to elucidate if this bond is a two-center three-electron (2c-3e) bond or a purely electrostatic interaction.

Let us therefore recall the definition of 2c-3e bonds, first described by Linus Pauling¹⁴ in the 1930s and attracted considerable attention in recent years. In molecular orbital (MO) terms, this type of bond is characterized by two electrons located in a bonding σ orbital and one electron in an antibonding σ^* orbital and is traditionally represented by the $\cdot\cdot$ symbol, introduced in the literature by Asmus.¹ Alternative names for this interaction are σ^* bond^{15–17} or hemi bond. Since the bond order is one-half or less, the dissociation energy of a 2c-3e bond is expected to be roughly half (or less) that of a 2c-2e bond and the bond distance should be longer than a corresponding 2c-2e bond. These predictions have proved to be correct in several prior studies of the one-electron reduction of lysozyme,¹⁸ of sulfur-containing radical ions,¹⁹ and of H_nX \cdot :YH_m⁻ radical anions (X, Y = Cl, S, P, F, O, N).²⁰ In the valence-bond (VB) formalism,¹⁴ the stability of the 2c-3e-bonded radical A \cdot :B results from a resonance between two limiting Lewis structures that are mutually related by a charge transfer as



where the eventual charge of the radical and of the fragments has not been indicated for the sake of generality. In such a resonance situation, the energy difference between the two limiting structures is of primary importance in determining the stabilization energy.

* Author to whom correspondence may be addressed. E-mail: fourre@lct.jussieu.fr.

[†] Université Pierre et Marie Curie.

[‡] Université René Descartes.

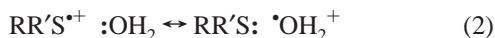
To distinguish between a 2c-3e bond or electrostatic interactions, we have chosen to carry out a comparative study of the S \cdots O bond for prototypical anion, cation, and neutral radicals (the \cdots notation will be used as long as the 2c-3e nature of the weak bond is not clearly established). These species are, respectively, the RSOH $^-$, the RR'SOH $_2^+$, and the RR'SOH radicals. We will first analyze the bonding for R and R' = H and then investigate the effect of methyl substitution on the sulfur center. From previous theoretical studies, the 2c-3e nature of the S \cdots O bond in the complexes is unambiguous.^{20,21} The cationic complexes, and more precisely the nonsubstituted¹⁶ and the disubstituted species,²² have been considered as three-electron-bonded radicals for a long time. However, recent calculations^{19,23} suggest that, for H $_2$ SOH $_2^+$, the lone electron is localized on the sulfur atom whereas, from the VB description (eq 1), a large resonance energy requires that the electron is delocalized between the two moieties. The topological analysis of the electron localization function,²⁴ already applied on 2c-3e radical anions,^{20,25} offers the opportunity of reinvestigating the formation of all these S \cdots O bonds. We will see that several topological criteria allow us to distinguish unambiguously the 2c-3e bond from the electrostatic one.

The organization of this paper is as follows: section II is dedicated to theoretical considerations, including the VB picture of the S \cdots O bond (II.A), the foundations of the topological analysis (II.B.1), its application to the 2c-3e bonds (II.B.2), and finally the calculation methods (II.C). Section III is devoted to the results; the applicability of the methods and basis sets is studied for perhydro-ionic species in section III.A, and the compared analysis of the nature of the S \cdots O bond in all the radicals is presented in section III.B. We present our conclusions in section IV.

II. Models, Concepts, and Methodology

II.A. VB Descriptions of the 2c-3e Bond S \cdots O Bond in Ionic and Neutral Radicals. The picture of the chemical bond provided by the VB formalism is generally easier to compare to the topological results than the MO picture. Thus the VB descriptions of the potential 2c-3e SO bonds in cation, anion, and neutral radicals, as well as the experimental difference in energy ΔE between the limiting Lewis structures, will be the starting point of this study.

For the eventual 2c-3e-bonded RR'S \cdots OH $_2^+$ cation radicals, the two VB structures may be the following



As first pointed out by Clark in his leading work on 2c-3e radical cations,¹⁷ the dissociation energy D_e of RR'S \cdots OH $_2^+$, i.e., the energy of the reaction



is expected to decrease exponentially as the difference in ionization potential between the fragments, $\Delta(\text{IP})$, increases, with $\Delta(\text{IP}) = \text{IP}(\text{H}_2\text{O}) - \text{IP}(\text{RR}'\text{S}) \sim \Delta E$.

The RS \cdots OH $^-$ anion radicals can be described by a resonance between the two following VB structures



By analogy with the cations, the dissociation energy D_e of RS \cdots OH $^-$, i.e., the energy of the reaction

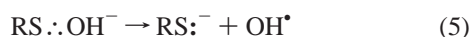


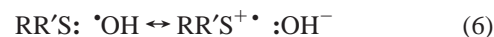
TABLE 1: Electron Affinities (EA) and Ionization Potentials (IP) of the Fragments and Their Difference, in eV

RSOH $^-$	EA(RS)	EA(OH)	$\Delta(\text{EA})$
HSOH $^-$	2.31 ^a	1.83 ^b	0.48
CH $_3$ SOH $^-$	1.87 ^c	1.83 ^b	0.04
RR'SOH $_2^+$	IP(H $_2$ O)	IP(RR'S)	$\Delta(\text{IP})$
H $_2$ SOH $_2^+$	12.65 ^d	10.46 ^e	1.19
HCH $_3$ SOH $_2^+$	12.65 ^d	9.45 ^f	3.20
(CH $_3$) $_2$ SOH $_2^+$	12.65 ^d	8.69 ^g	4.04
RR'SOH	IP(RR'S)	EA(OH)	IP-EA
H $_2$ SOH	10.46 ^e	1.83 ^b	8.63
HCH $_3$ SOH	9.45 ^f	1.83 ^b	7.62
(CH $_3$) $_2$ SOH	8.69 ^g	1.83 ^b	6.86

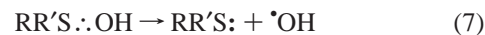
^a Reference 53. ^b Reference 54. ^c Reference 55. ^d Reference 56. ^e Reference 57. ^f Reference 58. ^g Reference 59.

is expected to decrease as the difference in electron affinity between the fragments $\Delta(\text{EA})$ increases, with $\Delta(\text{EA}) = \text{EA}(\text{RS}) - \text{EA}(\text{OH}) \sim \Delta E$.

For the neutral radicals, a 2c-3e S \cdots O bond would imply the existence of the following resonance



As already mentioned by McKee et al.,²⁶ the dissociation energy D_e of RR'S \cdots OH, i.e., the energy of the reaction



is expected to decrease as the difference between the IP of RR'S and the EA of H $_2$ O increases, with $\text{IP} - \text{EA} \sim \Delta E$.

The experimental values of IP, EA, and their differences are displayed in Table 1 and will be discussed in section III.B.2 together with our theoretical results.

II.B. The Topological Approach to the 2c-3e Bond.
II.B.1. Resume of the Topological Analysis of the Electron Localization Function (ELF) Gradient Field. The topological analysis of the ELF gradient field provides a mathematical model enabling the partition of the molecular position space into basins of attractors, which present in principle a one-one correspondence with chemical local objects such as bonds and lone pairs. These basins are either core basins, labeled C(X), which encompass the nuclei X with $Z > 2$, or valence basins, V(X, Y, ...), which fill the remaining space. The latter ones are characterized by their coordination number with core basins, which is the synaptic order. Monosynaptic basins thus correspond to conventional lone pairs, disynaptic basins to two-center bonds, and polysynaptic basins to multicenter bonds. Series of articles have been published concerning the theoretical foundations of this method^{24,27-31} or its applications to the understanding of the chemical structure of molecules and solids;^{28,32-41} thus here we will just recall some major points.

A localization domain is a region of space encompassed with an isoELF surface (a value around 0.8 is commonly chosen, delimiting volumes within which the Pauli repulsion is rather weak). It is called reducible when it contains more than one attractor. The bifurcation tree diagram describing the evolution of the localization domains with the ELF values is specific of the type of interactions in the molecular system. For example, it allows the build up of a scale for the weak and medium hydrogen bond by defining a core valence bifurcation (CVB) index, as introduced by Fuster and Silvi.³⁴ This index is negative when the first bifurcation creates two molecular-reducible domains (for weak H-bonded complexes) and positive when

the core–valence separation is the first bifurcation occurring in the reduction of the localization process (for medium H-bond complexes, which can thus be considered as single molecules).

Beyond this rather descriptive aspect, quantitative properties are further extracted by integrating the related property densities over the localization basins. For example, the integration of the one-electron density $\rho(\mathbf{r})$ inside a given basin Ω_a provides the average population of this basin and is conventionally denoted $\bar{N}(\Omega_a)$. When dealing with radicals, it is also informative to consider the integrated spin density

$$\langle S_z \rangle_{\Omega_a} = \frac{1}{2} \int_{\Omega_a} (\rho^\alpha(\mathbf{r}) - \rho^\beta(\mathbf{r})) d\mathbf{r} \quad (8)$$

which locates the unpaired electrons. For resonant bonds, of particular interest is the variance of the basin population which is a measure of the quantum mechanical uncertainty of the basin population. Its decomposition in terms of pair covariances²⁹ allows the definition of a topological index $\delta_{\Omega_a, \Omega_b}$, which is a measure of the delocalization between the basins Ω_a and Ω_b .²⁰

II.B.2. Topological Signatures of the Three-Electron Bond.

The topological ELF analysis has already been applied on disulfide anions²⁵ and on a series of anion radicals of the $H_nX \cdot : YH_m^-$ type, including $HS \cdot : OH^-$.²⁰ Three rules have been elaborated from these studies and a fourth one is added in this work:

1. There is no $V(X, Y)$ basin associated with a $X \cdot : Y$ bond, which can be interpreted as the effect of the Pauli repulsion of the two same-spin electrons (one in a σ orbital, the other in a σ^* orbital). In other words, the topology of 2c-3e-bonded complexes is composed of the union of the basins of the isolated fragments. Since the same pattern is obtained for all systems formed without electron pair sharing, as ionic and hydrogen-bonded complexes, some other rules are required to characterize the 2c-3e bond.

2. The extra electron density (and consequently the spin density) is mainly localized within the monosynaptic basins $V(X)$ and $V(Y)$. The strongest 2c-3e bonds are characterized by well-balanced sharing of the spin density between the two moieties.

3. The electron fluctuation between the two fragments, which is a central phenomenon in three-electron bonds, occurs mainly between the lone pairs of the two atoms X and Y. It can be quantified by the delocalization index $\delta_{V(X), V(Y)}$, which is maximal for homonuclear bonds and decreases as the difference in electronegativity of the fragments increases.

4. Similar to H-bonded complexes, a CVB index, $\vartheta(3e)$, can be defined for 2c-3e-bonded complexes $A \cdot : B$ (where A and B may be two molecular species), as

$$\vartheta(3e) = \eta(\mathbf{r}_{AB}) - \eta(\mathbf{r}_{cv}) \quad (9)$$

where $\eta(\mathbf{r}_{AB})$ is the value of the ELF at the saddle connection of the $V(A)$ and $V(B)$ monosynaptic basins of the two fragments and $\eta(\mathbf{r}_{cv})$ the lowest value of the ELF for which all the core basins of the composed system are separated from the valence. As it was suggested for $HS \cdot : SH^-$ by Bergès et al.,²⁵ the CVB indices of all $H_nX \cdot : YH_m^-$ radical anions are positive, which means that these complexes can be considered as single molecular species. More precisely, the values of $\vartheta(3e)$ range from 0.10 to 0.15 and decrease as the difference in electronegativity of the fragments increases. It is noteworthy that the CVB index should be considered as a semiquantitative one, since it is not related to integrated properties such as the basin populations.

II.C. Methods of Calculation. Concerning theoretical methods, several studies have shown that it is difficult to obtain a fully accurate description of the 2c-3e-bonded radical species. The most commonly used density functionals (including B3LYP) systematically fail to quantitatively describe these systems by overestimating the binding energies and the equilibrium distances as first shown by Braïda et al. for the cationic dimers $H_nX \cdot : XH_n^+$.⁴² This has been verified more recently by Carmichael for several perhydrido species σ^* -radical containing odd electron bonds as SS anions and cations, SN cations, and SO cations, from a variety of ab initio molecular orbital techniques and density functional theory.¹⁹ Only the BHLYP functional⁴³ provides equilibrium distances and dissociation energies of 2c-3e-bonded radical cations in good agreement with reference calculations or experimental results, except for the rare gas dimers.⁴⁴ However, the performances of this method with the 3e-bonded radical anions are much more erratic.⁴⁵ An alternative solution would be to optimize the radicals within the Møller–Plesset many-body perturbation theory at the second order (MP2). The MP2 method has been used for numerous cationic^{16,17} as well as for several anionic 3e-bonded radicals.⁴⁶ It has appeared to be the only candidate for calculating chemical properties of hemi-bonded species since it includes the essential dynamical correlation at a rather economical cost. However, Braïda et al. have brought to light and analyzed an unsuspected defect of the Møller–Plesset methods in the treatment of the 3e bonds, that is to say, the symmetry-breaking (for homonuclear 3e bonds) or near-symmetry-breaking artifact (for dissymmetric systems).^{21,47} In some cases, the predictions made at the MP2 level are even completely erroneous. When the MP_n approaches fail, one possible alternative for introducing dynamical correlation is the coupled-cluster theory, with inclusion of all single and double excitations and perturbative treatment of triple excitations (CCSD(T)).⁴⁸ However, because of its computational cost, this approach is applicable to small-model systems only, as those investigated in this paper. Thus, we will use the results of the coupled-cluster approach calculations as a benchmark against which to assess the reliability of MP2 and BHLYP methods. In view of possible applications to larger systems of biological interest, our choice should be the best compromise between efficiency and practicability.

III. Results and Discussion

III.A. Preliminary Study of the Nonsubstituted Ionic Radicals: Influence of Methods and Basis Sets. A double- ζ polarized basis is the required minimum for reproducing the dissociation energy of three-electron bonds, which should be augmented by diffuse functions for the anion and neutral radicals. The geometry optimizations of the nonsubstituted ionic radicals ($HSOH^-$ and $H_2SOH_2^+$) have been performed with three standard basis sets (6-31G*, 6-31+G*, and 6-311++G-(3df,2pd)) to examine whether the conclusions are dependent on basis-set improvements. With each basis set, the very accurate CCSD(T) level has been taken as the reference against which the other methods (MP2 and BHLYP) are evaluated. All the theoretical methods have been used in their spin-unrestricted forms. The frozen core approximation and the PMP2 level, which annihilate spin contamination by projection, have been used. We performed all the calculations with the Gaussian98 software.⁴⁹ The S–O equilibrium distances, resulting from a full optimization in every method/basis combination, are displayed in Table 2 and in Figure 1a. First, for the anion radical, we verify the requirement of introducing diffuse functions in the basis set: no geometry minimum is found at the BHLYP/

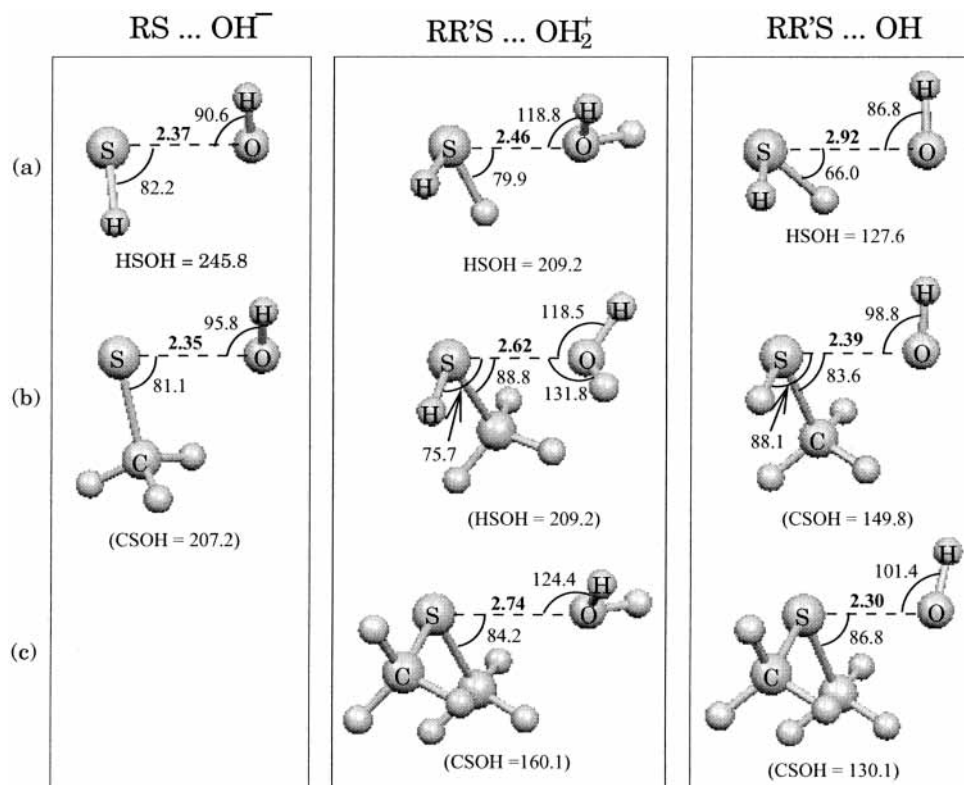


Figure 1. Optimized structures for the anionic, cationic, and neutral radicals (adducts) at the CCSD(T)/6-31+G* level for (a) R=R'=H, (b) R=H and R'=CH₃, and (c) R=R'=CH₃. The nonsubstituted systems have been fully optimized. For the substituted species, only the indicated coordinates have been optimized at the CCSD(T) level, the other ones being kept at their MP2 values (in parentheses). The distances are in Ångstroms, and the angles are in degrees.

TABLE 2: S–O Equilibrium Distance (in angstroms) for the Nonsubstituted Ionic Radicals Optimized at the BHLYP, MP2, and CCSD(T) Levels^a

species	BHLYP	MP2	CCSD(T)
HSOH ⁻	2.48	2.22	2.53
	2.46	2.17	2.37
H ₂ SOH ₂ ⁺	2.38	2.17	2.34
	2.41	2.39	2.42
	2.41	2.45	2.46
	2.41	2.40	2.42

^a For each system, the first line is obtained with the 6-31G*, the second one with the 6-31+G*, and the last one with the 6-311++G-(3df,2p) basis sets.

6-31G* level and, at the CCSD(T) level, a large shrinking (0.16 Å) of the distance is found when augmenting the basis from 6-31G* to 6-31+G*. Further improvement of the basis does not induce any noticeable modification of the bond length, whatever method is employed. Nevertheless, the structural features are very sensitive to the choice of the method. The bond length is found 0.12 Å too large at the BHLYP level, which indeed shows the erratic performances of this method mentioned above. The MP2 results are even worse, as it has been pointed out by Braïda et al. in a previous study on three-electron-bonded anion radicals.²¹ It is noteworthy that, since they are likely to overestimate the delocalization due to the self-interaction defect, the DFT methods are less sensible to this overlocalization of the charge. At contrast with HSOH⁻, the equilibrium structure of H₂SOH₂⁺ significantly depends neither on the method nor on the basis. Indeed, the 6-31G* basis set fulfills the minimum requirements recalled previously for describing 3e-bonded radical cations. Now for a given basis set, the bond distances provided by the BHLYP and the MP2 methods are both very close to the CCSD(T) result. This confirms on one hand the

ability of BHLYP to compensate the self-interaction error in cationic species and on the other hand the reliability of the unrestricted Hartree–Fock level in what concerns the description of the sharing of the positive charge among the two fragments. In view of the effect of the basis set on the structural parameters, we have chosen the 6-31+G* one for investigating the larger systems. Even though some weaknesses of the BHLYP and MP2 have been identified by studying the nonsubstituted systems, it is still difficult to choose between these methods so we continue with the three methods to study the neutral species. The MP2 and BHLYP structures have been fully optimized, as well as the CCSD(T) structures of the nonsubstituted radicals, whereas the CCSD(T) structures of the substituted species have only been partially optimized (Figure 1). Concerning the topological analysis of the ELF gradient field, the calculation of the variance of the basin population which is necessary to carry out the analysis of the delocalization, requires that the wave function is expressed in terms of a single determinant built on Hartree–Fock or Kohn–Sham orbitals. Thus, the wave function of each radical has been calculated at the BHLYP/6-31+G* level using the CCSD(T)/6-31+G* geometry. The TopMod package of programs developed in our laboratory⁵⁰ was then used to perform the calculation of the ELF on a grid, the partition of the molecular space into basins, their attribution, as well as the integration of the property densities described in section II.B.1.

III.B. Compared Analysis of the Nature of the S···O Bond in Ionic and Neutral Radicals. The following paragraphs are devoted to the detailed analysis of the S···O bond in the anionic, cationic, and neutral radicals. We begin with the RSOH⁻ radicals, which constitute our reference systems for the S···O 2c-3e bond. Then we investigate the RR'SOH₂⁺ complexes, which have been considered as 2c-3e-bonded systems since a long time. We then finish by the RR'SOH complexes, for which

TABLE 3: Variation of the Total Basin Population of the Sulfur-Centered Fragment with Respect to the Isolated Fragment for the Anionic, Cationic, and Neutral Radicals

Anion Radicals	$\Delta\bar{N}(\text{RS})$
HSOH ⁻	-0.47
CH ₃ SOH ⁻	-0.53
Cation Radicals	$\Delta\bar{N}(\text{RR}'\text{S})$
H ₂ SOH ₂ ⁺	0.15
HCH ₃ SOH ₂ ⁺	0.04
(CH ₃) ₂ SOH ₂ ⁺	0.03
Neutral Radicals	$\Delta\bar{N}(\text{RR}'\text{S})$
H ₂ SOH	-0.05
HCH ₃ SOH	-0.21
(CH ₃) ₂ SOH	-0.29

the nature of the S•••O bond will be established by comparison with the ionic complexes. In each case, we first analyze the structural and energetical parameters and then the results of the topological analysis. It is noteworthy that we adopt for the latter a different point of view than the one used in our previous paper on three-electron-bonded radical anions;²⁰ there we considered the formation of the three-electron bond as a result of an electron attachment, whereas now we compare the topology of the complex with those of both isolated fragments (RS and OH⁻ for the anions, RR'S⁺ and H₂O for the cations, and RR'S and OH for the neutral). In this context, it is interesting to investigate the global charge transfer from one fragment to another, resulting from the formation of the radical. For the anions, we thus define the variation of population of the sulfur-centered fragment $\Delta\bar{N}(\text{RS})$ as

$$\Delta\bar{N}(\text{RS}) = \bar{N}_{\text{comp}}(\text{RS}) - \bar{N}_{\text{iso}}(\text{RS}^-) \quad (10)$$

where $\bar{N}_{\text{comp}}(\text{RS})$ is the sum of the basin populations of the RS fragment in the RS•••OH⁻ 2c-3e-bonded complex and $\bar{N}_{\text{iso}}(\text{RS}^-)$ the sum of the basin populations of the isolated RS⁻ fragment (obviously $\Delta\bar{N}(\text{OH}) = -\Delta\bar{N}(\text{RS})$). Similar quantities can be calculated for the cation and neutral radicals, and the results obtained for all the species under scrutiny are gathered in Table 3.

III.B.1. The RSOH⁻ Anion Radicals. As already mentioned by Braïda et al., “the RS (R = H, CH₃) and OH fragments are good candidates for fragments that could possibly form 2c-3e-bonded anions RS•••OH⁻ because they are good electron acceptors and display comparable EA”.²¹ We enlarge their study by examining the dissociation energies and the topological features of these species. The S–O bond lengths and the dissociation energies of HSOH⁻ and CH₃SOH⁻ as obtained with the three methods are reported in Table 4 together with the results of previous works. What has been said in the previous paragraph concerning the weakness of the MP2 and BHLYP methods for the prediction of the equilibrium geometries remains valid for the substituted systems: the bond length remains too short at the MP2 level and too long at the BHLYP level. However, the effect of substitution, though in the opposite sense for both methods (the MP2 bond length increasing and the BHLYP one decreasing), leads to values of the S–O distance closer to the one obtained within the reference CCSD(T) method. One notices that the substitution has nearly no effect on the CCSD(T) S–O bond length, which decreases by only 0.02 Å. The corresponding structures are depicted in Figure 1a, together with relevant geometrical data. We note differences with the previous results,²¹ essentially on the angles, due to the full geometry relaxation. Despite the absence of variations of

TABLE 4: Structural and Energetical Parameters of the Anion, Cation, and Neutral Radicals^a

species	BHLYP		MP2		CCSD(T)		lit	
	R _e	D _e	R _e	D _e	R _e	D _e	R _e	D _e
HSOH ⁻	2.48	15.7	2.17	22.1	2.37	20.2	2.38 ^b	
CH ₃ SOH ⁻	2.42	19.9	2.23	29.4	2.35	25.5	2.35 ^b	
H ₂ SOH ₂ ⁺	2.41	24.7	2.45	22.6	2.46	22.4	2.42 ^c	23.7 ^c
							2.46 ^d	21.7 ^d
							2.437 ^e	
							2.454 ^f	
								23.8 ^g
HCH ₃ SOH ₂ ⁺	2.54	18.7	2.60	18.7	2.62	18.3		
(CH ₃) ₂ SOH ₂ ⁺	2.68	15.1	2.73	16.0	2.74	15.7	2.88 ^h	16.8 ^h
H ₂ SOH	2.80	3.2	3.12	3.0	2.92	3.4	2.517 ⁱ	0.2 ^j
HCH ₃ SOH	2.57	4.5	2.11	3.5	2.39	5.0	2.393 ⁱ	2.9 ^j
(CH ₃) ₂ SOH	2.42	6.4	2.07	8.6	2.30	8.4	2.326 ⁱ	7.4 ^j
							2.047 ^j	9.3 ^j
								8.7 ^k

^a R_e is the S–O equilibrium distance in angstroms, and D_e is the dissociation energy of the complex (see text) in kcal mol⁻¹. The calculations have been carried out using the 6-31+G* basis set. Symmetric species have been optimized within C_s symmetry. ^b CCSD(T)/6-31+G(d).²¹ ^c BHLYP/6-31++G(d,p).²³ ^d MP2/6-31++G(d,p).²³ ^e MP2/6-311G(2d,p).¹⁹ ^f QCISD/6-311G(2d,p).¹⁹ ^g MP2/6-31G(d).¹⁶ ^h HF/6-31G(d).²² ⁱ B3LYP/cc-pVTZ (G2 method).¹⁰ ^j MP2/6-31+G(2d).⁷ ^k QCISD(T)/6-31+G(2d)//MP2/6-31+G(2d).⁷

the bond length under substitution, there is a significant increase of the dissociation energy from 20.2 to 25.5 kcal mol⁻¹. It is noteworthy that, in contrast with the discrepancies observed for the bond lengths, the MP2 predictions of D_e are in surprisingly good agreement with the CCSD(T) ones, as already mentioned by Braïda et al. in the case of the dihalogen radical anions.²¹ In return, the BHLYP values are underestimated, in agreement with the overestimation of the equilibrium distance. Finally this strengthening of the bond, which was expected from the decrease of ΔEA (see Table 1), could result from the electron release of the methyl group; indeed, if one considers the formation of RS•••OH⁻ by the approach of RS:•⁻ and •OH, the substitution takes place on the fragment that bears the lone pair; the ability of RS:•⁻ to transfer electron density toward the hydroxyl fragment may thus be enhanced.

On a topological point of view, the RSOH⁻ anions verify the first of the four rules recalled in the previous section (i.e., absence of disynaptic basin between the two moieties in interaction), as shown in Figure 2a for HSOH⁻. It is worthy to note the lateral orientation of the lone pairs basins of the two interacting atoms, in view of the comparison with the cationic and neutral systems. Let us now consider the quantitative topological properties. First, on a global point of view, the formation of the HS•••OH⁻ anion radical is accompanied by a charge transfer of 0.47 e from the HS⁻ to the OH fragment whereas for CH₃S•••OH⁻ the charge transfer is equal to 0.53 e, as shown by the variations of the gross population of the RS fragment displayed in Table 3. This charge transfer occurs mainly between the lone pairs of the interacting atoms; thus only the integrated properties of the monosynaptic basins have been reported in Table 5. Concerning the isolated fragments, the population \bar{N} of the V(O) basin (5.28 vs 5.0 e from the Lewis structure of •OH) reflects the large electronegativity of the oxygen atom, whereas the population of V(S) in HS⁻ is in better agreement with the three lone pairs of its Lewis structure. It increases by 0.06 e in CH₃S⁻ due to the electron-releasing character of the CH₃ substituent. It is noteworthy that the ⟨S_z⟩ value of V(O) corresponds to 84% of the spin density, the missing 16% being distributed among V(H,S) (11%) and C(S)

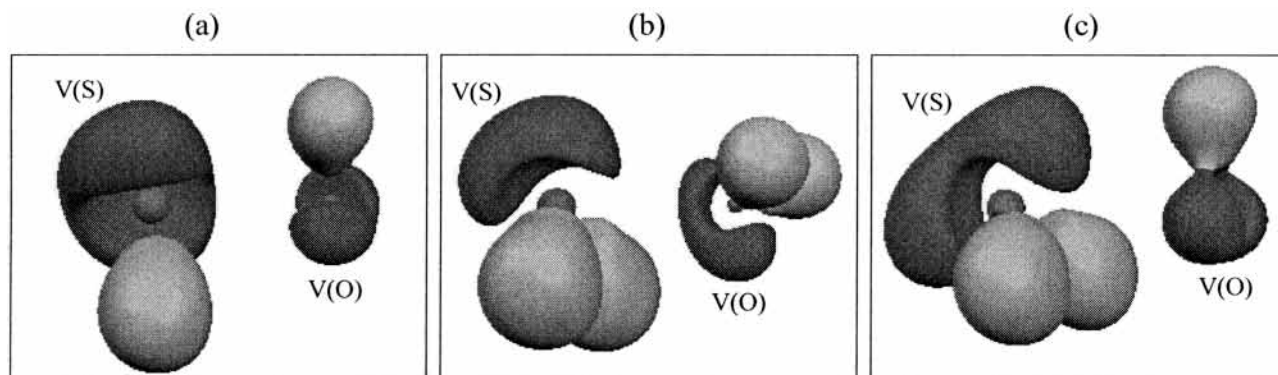


Figure 2. ELF isosurfaces for (a) HSOH^- , (b) H_2SOH_2^+ , and (c) H_2SOH . Actually, for all the radicals, the V(O) basin corresponds to the union of two monosynaptic basins whereas the V(S) basin corresponds to the union of two monosynaptic basins only for the anions and the neutral radicals.

TABLE 5: Topological Parameters of the Anion, Cation, and Neutral Radicals and Their Fragments (BHLYP/6-31+G* Single-Point Energy Calculation at the CCSD(T)/6-31+G* Geometry)^a

	V(S)		V(O)		$\delta_{V(S),V(O)}$	$\vartheta(3e)$
	\bar{N}	$\langle S_z \rangle$	\bar{N}	$\langle S_z \rangle$		
OH			5.28	0.42		
HS^-	6.12					
CH_3S^-	6.18					
HSOH^-	5.61	0.21	5.73	0.23	0.58	0.13
CH_3SOH^-	5.62	0.24	5.82	0.20	0.54	0.14
OH_2			4.71			
H_2S^+	2.94	0.34				
HCH_3S^+	3.08	0.34				
$(\text{CH}_3)_2\text{S}^+$	3.19	0.33				
H_2SOH_2^+	3.07	0.30	4.45	0.06	0.22	0.06
$\text{HCH}_3\text{SOH}_2^+$	3.08	0.31	4.60	0.02	0.12	-0.02
$(\text{CH}_3)_2\text{SOH}_2^+$	3.17	0.32	4.61	0.02	0.10	-0.04
H_2S	4.32					
HCH_3S	4.38					
$(\text{CH}_3)_2\text{S}$	4.46					
H_2SOH	4.26	0.02	5.31	0.40	0.12	-0.07
HCH_3SOH	4.05	0.10	5.45	0.32	0.38	0.07
$(\text{CH}_3)_2\text{SOH}$	4.00	0.13	5.52	0.28	0.48	0.13

^a Population is \bar{N} , integrated spin density of the monosynaptic basins V(S) and V(O) is $\langle S_z \rangle$, index of delocalization between these two basins is $\delta_{V(S),V(O)}$, and the CVB Index is $\vartheta(3e)$.

(5%). When $\text{HS} \cdot \text{OH}^-$ is setting, the V(S) population decreases by 0.51 e whereas the V(O) population increases by 0.45 e. This discrepancy from the global value results from small rearrangements between the other basins. A quasiequal sharing of the spin density among the lone pairs of the two fragments is thus obtained, as specified by the rule $n^\circ 2$, the V(O) basin being only slightly preferred. This gives rise to a large value of the delocalization index $\delta_{V(S),V(O)}$, consistent with the rule $n^\circ 3$. Indeed, values of δ around 0.6 are typical for $\text{H}_n\text{X} \cdot \text{YH}_m^-$ 3e-bonded radical anions, the largest one being obtained for the homonuclear complex $\text{Cl} \cdot \text{Cl}^-$, with $\delta = 0.7$. Finally the positive value of $\vartheta(3e)$, 0.13, is in agreement with the rule $n^\circ 4$. The investigation of the substitution of H by CH_3 on the sulfur atom leads to the following remarks:

1. The V(S) population remains unchanged contrary to the V(O) one, which is enhanced by 0.09 e. The electron-releasing character of the methyl group thus results in a greater electron transfer from the sulfur atom to the more electronegative oxygen atom, which might explain the stabilization of the anion under substitution.

2. The integrated spin densities remain quasiequally shared among V(S) and V(O), which means that both VB structures of resonance (4) are nearly equiprobable. The small variations of $\delta_{V(S),V(O)}$ and $\vartheta(3e)$ result from the strategy adopted for the topological analysis (BHLYP single-point calculation on the CCSD(T) geometry) and, consequently, can be neglected.

III.B.2. The $\text{RR}'\text{SOH}_2^+$ Cation Radicals. One notices that, as for H_2SOH_2^+ , the two approximate methods, and especially the MP2 one, provide bond lengths for the substituted systems which are in very good agreement with the reference CCSD(T) ones (see Table 4). Conversely to the anions' case, the substitution has a large effect on the S–O distance, which increases by 0.16 Å from H_2SOH_2^+ to $\text{HCH}_3\text{SOH}_2^+$ and by 0.12 Å from $\text{HCH}_3\text{SOH}_2^+$ to $(\text{CH}_3)_2\text{SOH}_2^+$ in the CCSD(T) framework. The corresponding structures are depicted in Figure 1b, together with pertinent geometrical data. Though the $\text{H}\hat{\text{S}}\text{O}$ or $\text{C}\hat{\text{S}}\text{O}$ valence angles are similar to the ones obtained for the radical anions, the $\text{H}\hat{\text{O}}\text{S}$ angles are much larger, ranging from about 118° to 124°. However, in 2c-3e-bonded systems, typical values of the valence angles range from 80 to 110° (see Figure 1 for the anions and ref 47 for the cations) and thus favor an efficient overlap of the lone pairs of the two interacting fragments. Concomitantly, with the increase of the S–O distance, the dissociation energy decreases by methyl substitution. This was expected from the increase of $\Delta(\text{IP})$ (see Table 1). Furthermore these values are very large as compared to the $\Delta(\text{EA})$ of the anions and should not favor the resonance (2). Similarly as in the anions' case, the weakening of the bond could also be understood by the electron releasing of the methyl group; however, the effect is reversed because the methyl substitution does not take place on the fragment that bears the lone pair. The comparison with the results of previous reports, gathered in Table 4, shows that the bond energy of the nonsubstituted system, as the equilibrium structure, is weakly dependent on the chosen method/basis set combination. For $(\text{CH}_3)_2\text{SOH}_2^+$, where the HF/6-31G(d) dissociation energy is surprisingly correct, the bond length is overestimated. These results do not correspond to the expected performances of the HF method on 2c-3e complexes, which are to provide qualitatively correct geometry and largely underestimated bond energy.⁵¹ Finally, though the bond lengths and energies are consistent with what is expected for 2c-3e-bonded radical cations, several indices, as large $\Delta(\text{IP})$ or large valence angles, make the 2c-3e nature of the $\text{S} \cdot \cdot \text{O}$ bond in the $\text{RR}'\text{SOH}_2^+$ complexes questionable.

The qualitative topological description is provided by the ELF isosurface, which is displayed for H_2SOH_2^+ in Figure 2b. The rule $n^\circ 1$ is verified for this cation as well as for the substituted ones. The presence of two protonated disynaptic basins con-

TABLE 6: Localization ($\langle S_z \rangle$) and Delocalization (δ) Topological Parameters, as Well as the CVB Index for the $H_2XYH_2^+$ Cation Radicals (X, Y = S, O)^a

$H_2XYH_2^+$	$\langle S_z \rangle_{V(X)}$	$\langle S_z \rangle_{V(Y)}$	$\delta_{V(X),V(Y)}$	$\delta_{X,Y}$	$\vartheta(3e)$
$H_2S\cdots OH_2^+$	0.30	0.06	0.22	0.40	0.06
$H_2O\cdots OH_2^+$	0.17	0.17	0.28	0.56	0.18
$H_2S\cdots SH_2^+$	0.19	0.19	0.36	0.64	0.20

^a $\delta_{X,Y}$ quantifies the electron delocalization between all the basins of the H_2X^+ and the H_2Y moieties.

nected to C(S) as well as to C(O) results in a relative axial orientation of the lone-pair basins of the interacting S and O atoms. This has to be compared to the lateral orientation in the anionic systems, which could appear as the optimal one for the electron fluctuation. More quantitative topological properties will lead us to a firm conclusion concerning the nature of the $S\cdots O$ bond in the radical cations. As shown by Table 3, the formation of the radical gives rise to a global charge transfer of 0.15 e from the H_2O to the H_2S^+ fragment, namely, in the opposite direction than in the anions. This transfer is nearly nonexistent for the substituted systems. The data of Table 5 bring to light in more details the differences between the cases of the cations and anions. At first, concerning the fragments, the V(O) population in H_2O , as compared to the V(S) population in H_2S , reflects the larger electronegativity of the oxygen atom. Moreover, the increase of the V(S) population by methyl substitution reveals the electron releasing of the methyl substituent. It is worthy to note the rather small contribution (68%) of V(S) to the total spin density, mainly due to the presence of two protonated V(H,S) basins. In consequence of the formation of the $S\cdots O$ bond in $H_2SO_2^+$, the V(O) population decreases by 0.26 e, among which 0.11 flow into the V(O,H) basins. The fact that the lone pair is provided by the fragment containing the most electronegative atom might explain this weak rearrangement. As a result, the spin density remains essentially localized on the sulfur atom, and that involves a small electron delocalization between the V(S) and V(O) basins, $\delta_{V(S),V(O)} = 0.22$, to be compared with about 0.6 in the radical anions. The CVB index is positive but very low as compared to the case of the anions. These topological results are somehow surprising considering the moderate value of the $\Delta(IP)$ index. So it is interesting to compare the topological parameters of $H_2SOH_2^+$ with the equivalent ones in the typical 2c-3e-bonded radical cations $H_2O\cdots OH_2^+$ and $H_2S\cdots SH_2^+$ (see Table 6). Because of the large number of protonated basins in these three cations, a better picture of the electron delocalization is obtained by considering a global $\delta_{X,Y}$ index where X and Y, respectively, represent all the basins of the H_2X^+ and H_2Y fragments. For $H_2SOH_2^+$, the electron delocalization remains rather small ($\delta_{S,O} = 0.40$). For $H_2O\cdots OH_2^+$ and $H_2S\cdots SH_2^+$, though the delocalization between the monosynaptic basins alone remains moderate, the $\delta_{O,O}$ and $\delta_{S,S}$ values, as well as the $\vartheta(3e)$ ones, corroborate the 2c-3e nature of the O \cdots O and S \cdots S bonds. This is not the case for the $S\cdots O$ bond, which does not verify the rules n° 2, 3, and 4. Our conclusions, based on a topological approach, also agree with the results of Maity,²³ who investigated the nature of the binding in the radical cation complexes $H_nX\cdots YH_m^+$ by a population-based localization procedure applied to the highest doubly occupied molecular orbital. He showed that, for $H_2SOH_2^+$ and some other disymmetric cations, there was no orbital overlapping, contrary to all the symmetric species.

The substitution amplifies the localization of the extra electron in the V(S) basin, and consequently still lowers the delocalization index. This was expected from the increase of $\Delta(IP)$. Finally

$\vartheta(3e)$ becomes negative, which means that in $HCH_3SO_2^+$ and $(CH_3)_2SOH_2^+$, the two fragments keep their individuality. Therefore, the 2c-3e-type interaction, even in $H_2SOH_2^+$, is only a minor contribution of the bonding, which should be best described by an electrostatic interaction, this latter contribution increasing with the substitutions. We have now to our disposal some structural and topological data for the 2c-3e S \cdots O interaction in the radical anion complexes, and for the mainly electrostatic interaction $S\cdots O$ in the radical cation complexes. So we will investigate the nature of the $S\cdots O$ bond in the neutral radical complexes.

III.B.3. The RR'SOH Neutral Radicals. First, one notices that H_2SOH presents very specific features, because its S—O distance is surprisingly large whatever is the method of calculation (see Table 4): 2.92 Å within CCSD(T), which is intermediate between 2.80 Å (BHLYP) and 3.12 Å (MP2). The CCSD(T) structure is depicted in Figure 1a, and it is interesting to compare it with the structures of HSO^- and $H_2SOH_2^+$. In both species the interaction is mainly between the S and O atoms, which point toward each other, whereas in the neutral one, the hydrogen atoms of the H_2S fragment are directed toward the oxygen of the hydroxyl group ($HSO = 66.0^\circ$). The reason could be that this complex is stabilized by a hydrogen bond or a van der Waals interaction and not by a 2c-3e S \cdots O bond. This effect was noticed earlier²⁵ when comparing the radical anion $HS\cdots HS^-$ to its protonated derivative H_3S_2 . Conversely to the bond length, D_e is not sensitive to the method of calculations we employed and is very low, around 3 kcal mol⁻¹.

Second, after one substitution, the S—O distance dramatically shrinks, which might indicate a change in the nature of the bond. For both substituted species, many similarities occur between the neutral radicals and the anions. For instance, the BHLYP and MP2 values keep enclosing the CCSD(T) ones, but the BHLYP distance is now closer to the CCSD(T) one. Moreover, the CCSD(T) geometries depicted in parts b and c of Figure 1 are consistent with the one of the 2c-3e-bonded radicals. Also, we notice that the MP2 dissociation energies are in good agreement with the reference CCSD(T) ones, especially for the disubstituted species. Nevertheless, these D_e remain rather low. If we focus our attention on the relation with the experimental data, we notice that the IP-EA values are larger than the $\Delta(IP)$ ones and much more larger than the $\Delta(EA)$ ones. Thus, at first glance, the situation does not seem very favorable for the formation of a three-electron bond between RR'S and the $\bullet OH$ radical. These large IP-EA values for the RR'SOH radicals may explain the small values of D_e . However, McKee et al. have characterized 2c-3e-bonded systems formed by addition between the Cl \bullet radical and nitrogen bases, for which the IP-EA index reaches 6.5 eV.²⁶ This is not so far from the lowest value (6.9 eV) obtained for $(CH_3)_2SOH$. By substitution, D_e increases up to 8.4 kcal mol⁻¹, as expected from the diminution of IP-EA. Though this strengthening of D_e is similar to the one observed for the anions with $\Delta(EA)$, we notice that it follows the shortening of the bond length.

Our results for the most-studied disubstituted radical are in agreement with the first ones of McKee,⁷ but they are somewhat contradictory with those of Tureček^{9,52} and of Wang and Zhang.¹⁰ Whatever method we used, we always obtained 2c-3e-type structures, whereas Tureček and Wang and Zhang found different structures depending of the calculation method. Within an MP2 framework, they obtained a structure with the H atom of the OH moiety pointing to the S atom of the DMS moiety stabilized by a "dipole-dipole"-type interaction. The discrepancies between our frozen-core MP2 and the full MP2 results

of Tureček are not due to our approximation since we have verified that inclusion of core electrons into the basis set leads to the same 2c-3e structure. Within a B3LYP/cc-pVTZ framework, these authors obtained both structures. Surprisingly, the 2c-3e structure obtained by Wang and Zhang is in good agreement with our CCSD(T)/6-31+G* one. In that case, it seems that using very large basis set, but without the diffuse functions required by the resonance (6), balances the inherent inadequacy of this DFT method.⁴² Hence, we had eliminated the B3LYP method after preliminary calculations with the three standard basis sets (mentioned in section III.A) because we had pointed out the well-known overestimation of the dissociation energy.

Furthermore, we will also compare our results on the mono- and nonsubstituted radicals with the 2c-3e structures of Wang and Zhang using the B3LYP method. The energy and geometry of the monosubstituted radical are close to our CCSD(T) results, as for the DMS. However, for H₂SOH, Wang and Zhang have found a very weakly bonded structure ($D_e = 0.2 \text{ kcal mol}^{-1}$), the S–O bond length being 2.517 Å, which is far from our result discussed previously. It must be noted that, even after full optimization at the CCSD(T)/6-311++G(3df,2pd) level, we still get a large S–O bond length of 2.83 Å.

The topological results will help us to characterize the nature of the S•••O bond in the neutral radicals. At first, their ELF isosurface still verifies the rule $n^\circ 1$, as shown in Figure 2c for the simplest H₂SOH. For the three neutral radicals, it is worthy to note the “T” orientation of these basins, intermediate between the lateral one observed in the anions and the axial one observed in the cations. For the quantitative analysis, we must differentiate the nonsubstituted and substituted species, as it was noted for the structural and energetical results. As shown by Table 3, H₂SOH behaves as the substituted radical cation since there is nearly no charge transfer between the monosynaptic basins. The detailed analysis, see Table 5, shows that the V(O) and V(S) populations are not modified when the S•••O bond is setting. Consequently, the electron remains mainly localized into the V(O) basin as indicated by the $\langle S_z \rangle$ value of 0.4. The low delocalization index and the negative $\vartheta(3e)$ definitively corroborate the electrostatic nature of the S•••O bond, as in the substituted radical cations. In return, the topological parameters of the substituted species show several similarities with those of the anion radicals. As shown by Table 3, there is a nonnegligible charge transfer from the RCH₃S to the OH fragment in the substituted radicals, increasing from 0.21 e in HCH₃SOH to 0.29 e in (CH₃)₂SOH. From the population analysis of Table 5, it can be deduced that the charge transfer mainly occurs from the V(S) to the V(O) basin (there is a discrepancy between the global charge transfer and the variations of the basin populations because of the flow of population to the V(H,S) basin and to the V(S,C) one(s)). As a consequence of this greater charge transfer, the $\langle S_z \rangle$ value of the V(S) basin decreases and reaches 0.28 in the disubstituted radical. Also, the balancing of the spin density gives rise to an increase of the delocalization index, up to 0.48 in the DMS•••OH, and in the CVB index, up to 0.13, which is the same value as in the anions. It is noteworthy that the evolution of the topological features under substitution is consistent with the decrease of the IP-EA index. Finally, these topological results bring into light the intermediate nature of the S•••O bond in the substituted radicals; it is an interaction essentially electrostatic in HCH₃SOH but 2c-3e-bonded in DMS•••OH.

IV. Conclusion

Some criteria are proposed to differentiate a 2c-3e bond from an electrostatic interaction and are applied to the anion RS•••OH[−], the cation RR'S•••OH₂⁺, and the neutral RR'S•••OH radicals. First, the experimental difference in energy between the limiting VB structures, that is, $\Delta(\text{IP})$ for the cations, $\Delta(\text{EA})$ for the anions, and IP-EA for the neutrals, is used as an “energetical index” for the existence of a three-electron bond. From the small values of $\Delta(\text{EA})$, only the RS•••OH[−] anion radicals present such a 2c-3e bond. So a set of five criteria was determined from the topological study of the anionic species to characterize this type of bond. The absence of a disynaptic basin is a qualitative criterion, which is a common feature for all interactions without electron pair sharing. It is thus complemented by a semiquantitative one, the CVB index $\vartheta(3e)$, which is positive for a 2c-3e-bonded complex and around 0.13 for the S•••O bond. The radical anions evidently and, among the neutral radicals, the DMS•••OH species verify these two rules, contrary to the RR'S•••OH₂⁺ radical cations. The quantitative criteria allow us to specify (i) the charge transfer, ΔN , between the fragments involved in the formation of the S•••O bond, (ii) the sharing of the spin density $\langle S_z \rangle$, and (iii) the electron delocalization $\delta_{V(S),V(O)}$ between the V(S) and V(O) monosynaptic basins. For the anions (respectively, for the substituted neutrals), the charge transfer occurs from the sulfur-centered fragment to the hydroxyl fragment and reaches 0.5 e (respectively, 0.3 e). For the cations, the transfer is very low and occurs from H₂O to the sulfur-centered fragment. In all these radicals, as it was already shown for radical anions,²⁰ the spin density is mainly localized within the monosynaptic basins. However, only well-balanced values characterize the pure odd-electron bond and give rise to a large delocalization index, like 0.58 for the anions and 0.48 for DMS•••OH, whereas the maximum value for the cations is 0.22. The topological analysis allows us to calculate the weights of the limiting VB structures by summing the $\langle S_z \rangle$ values over the whole basins of each fragment; for the anions (see resonance (4)), it gives rise to equally probable structures, whereas for the cations, the RR'S••••OH₂ structure (see resonance (2)) is always the dominant one, from 84% for H₂SOH₂⁺ up to 96% for the disubstituted species. For the neutral radicals, the nature of the S•••O interaction is modified by substitution; it is clearly of the van der Waals type in H₂SOH, with the neutral H₂S:•OH structure (see resonance (6)) contributing to 96%, and mainly of the 2c-3e type in the disubstituted species, the same structure contributing to 66%, whereas in the monosubstituted one there is a balance of both interactions.

Afterward, we can conclude that, besides the energetical index, topological criteria must be taken into account in order to characterize a 2c-3e-bonded structure. Hence, the disubstituted neutral radical, despite a low dissociation energy D_e , presents such a 2c-3e S•••O bond. Furthermore, from a chemical point of view, the stabilizing effects of the substituents were pointed out for the formation of the three-electron bond as well as for the anions and the neutral radicals.

By comparison with predictions from accurate CCSD(T) calculations in some simple model systems, B3LYP and MP2 are shown to have difficulties for correctly describing the electronic structure of these radicals, more specifically neutral and anionic ones. Furthermore, knowing the systematic behaviors uncovered in such comparative studies then allows calculations within low-level methods using small basis sets to be cautiously applied to larger, presumably more chemically or

biologically interesting, compounds, for which the CCSD(T) treatment is computationally too demanding.

Acknowledgment. This work has been supported by the CNRS (UMR7616) and the French National Computing Center (IDRIS) in Orsay. We are indebted to B. Braïda for fruitful discussions and P. Reinhardt for his critical reading of the manuscript.

References and Notes

- (1) Asmus, K. D. *Acc. Chem. Res.* **1979**, *12*, 436.
- (2) Asmus, K. D. In *Sulfur-Centered Reactive Intermediates in Chemistry and Biology*; Chatgililoglu, C., Asmus, K. D., Eds.; Plenum Press: New York, 1990; pp 155–172.
- (3) Asmus, K. D. *Nukleonika* **2000**, *45*, 3.
- (4) Armstrong, A. D. In *S-Centered Radicals*; Alfassi, Z. B., Ed.; John Wiley & Sons, Ltd: New York, 1999; Chapter 2.
- (5) Schöneich, C.; Bobrowski, K. *J. Am. Chem. Soc.* **1993**, *115*, 6547.
- (6) Hynes, A. J.; Wine, P. H.; Semmes, D. H. *J. Phys. Chem.* **1986**, *90*, 4148.
- (7) McKee, M. L. *J. Phys. Chem.* **1993**, *97*, 10971.
- (8) Marciniak, C.; Bobrowski, K.; Hug, G. L.; Rozwadowski, J. *J. Phys. Chem.* **1994**, *98*, 4854.
- (9) Tureček, F. *J. Phys. Chem.* **1994**, *98*, 3701.
- (10) Wang, L.; Zhang, J. *J. Mol. Struct.* **2001**, *543*, 167.
- (11) Hynes, A. J.; Stoker, R. B.; Pounds, A. J.; McKay, T.; Bradshaw, J. D.; Nicovich, J. M.; Wine, P. H. *J. Phys. Chem.* **1995**, *99*, 16967.
- (12) Chatgililoglu, C.; Castelhana, A. L.; Griller, D. *J. Org. Chem.* **1985**, *50*, 2516.
- (13) Chatgililoglu, C. In *The Chemistry of Sulphenic acids and their Derivatives*; Patai, S., Ed.; John Wiley & Sons, Ltd: New York, 1990; pp 549–569.
- (14) Pauling, L.; MacClure, V. *J. Am. Chem. Soc.* **1931**, *53*, 3225.
- (15) Baird, N. C. *J. Chem. Educ.* **1977**, *54*, 291.
- (16) Clark, T. *J. Am. Chem. Soc.* **1988**, *110*, 1672.
- (17) Gill, P. M. W.; Radom, L. *J. Am. Chem. Soc.* **1988**, *110*, 4931.
- (18) Bergès, J.; Kassab, E.; Conte, D.; Adjadj, E.; Houée-Levin, C. *J. Phys. Chem.* **1997**, *101*, 7809.
- (19) Carmichael, I. *Nukleonika* **2000**, *41*, 11.
- (20) Fourré, I.; Silvi, B.; Sevin, A.; Chevreau, H. *J. Phys. Chem. A* **2002**, *106*, 2561.
- (21) Braïda, B.; Hiberty, P. *J. Phys. Chem. A* **2000**, *104*, 4618.
- (22) Clark, T. In *Sulfur-Centered Reactive Intermediates in Chemistry and Biology*; Chatgililoglu, C., Asmus, K. D., Eds.; Plenum Press: New York, 1990; pp 13–18.
- (23) Maity, D. K. *J. Phys. Chem. A* **2002**, *106*, 5716.
- (24) Silvi, B.; Savin, A. *Nature* **1994**, *371*, 683.
- (25) Bergès, J.; Fuster, F.; Silvi, B.; Jacquot, J.; Houée-Levin, C. *Nukleonika* **2000**, *45*, 23.
- (26) McKee, M. L.; Nicolaidis, A.; Radom, L. *J. Am. Chem. Soc.* **1996**, *118*, 10571.
- (27) Becke, A. D.; Edgecombe, K. E. *J. Chem. Phys.* **1990**, *92*, 5397.
- (28) Savin, A.; Nesper, R.; Wengert, S.; Fässler, T. F. *Angew. Chem., Int. Ed. Engl.* **1997**, *36*, 1809.
- (29) Noury, S.; Colonna, F.; Savin, A.; Silvi, B. *J. Mol. Struct.* **1998**, *450*, 59.
- (30) Silvi, B. *J. Mol. Struct.* **2002**, *614*, 3.
- (31) Silvi, B. *J. Phys. Chem. A* **2003**, *107*, 3081.
- (32) Fourré, I.; Silvi, B.; Chaquin, P.; Sevin, A. *J. Comput. Chem.* **1999**, *20*, 897.
- (33) LLusar, R.; Beltrán, A.; Andrés, J.; Noury, S.; Silvi, B. *J. Comput. Chem.* **1999**, *20*, 1517.
- (34) Fuster, F.; Silvi, B. *Theor. Chem. Acc.* **2000**, *104*, 13.
- (35) Chevreau, H.; Sevin, A. *Chem. Phys. Lett.* **2001**, *322*, 9.
- (36) Choukroun, R.; Donnadiou, B.; Zhao, J.-S.; Cassoux, P.; Lepetit, C.; Silvi, B. *Organometallics* **2000**, *19*, 1901.
- (37) Silvi, B.; Gatti, C. *J. Phys. Chem. A* **2000**, *104*, 947.
- (38) Fressigné, C.; Madaluno, J.; Giessner-Prettre, C.; Silvi, B. *J. Org. Chem.* **2001**, *66*, 6476.
- (39) Noury, S.; Silvi, B.; Gillespie, R. J. *Inorg. Chem.* **2002**, *41*, 41.
- (40) Lepetit, C.; Silvi, B.; Chauvin, R. *J. Phys. Chem. A* **2003**, *107*, 464.
- (41) Pilmé, J.; Silvi, B.; Alikhani, M. E. *J. Phys. Chem. A* **2003**, *107*, 4506.
- (42) Braïda, B.; Hiberty, P.; Savin, A. *J. Phys. Chem. A* **1998**, *102*, 7872.
- (43) Becke, A. D. *J. Chem. Phys.* **1993**, *98*, 1372.
- (44) The Gaussian key word for this functional is bhandhlyp.
- (45) Braïda, B., Étude theorique des liaisons à trois électrons dans les ions radicaux, Ph.D. Thesis, Université Paris-Sud, Orsay, France, September 2002.
- (46) Humbel, S., Ph.D. Thesis; Université Paris-Sud, Orsay, France, 1995.
- (47) Braïda, B.; Lauvergnat, D.; Hiberty, P. *J. Chem. Phys.* **2001**, *115*, 90.
- (48) The single excitations play an important role in the orbital relaxation, and the triple excitations are required for the calculation of energy differences.
- (49) Frisch, M. J.; Trucks, G. W.; Schlegel, H. B.; Scuseria, G. E.; Robb, M. A.; Cheeseman, J. R.; Zakrzewski, V. G.; Montgomery, J. A., Jr.; Stratmann, R. E.; Burant, J. C.; Dapprich, S.; Millam, J. M.; Daniels, A. D.; Kudin, K. N.; Strain, M. C.; Farkas, O.; Tomasi, J.; Barone, V.; Cossi, M.; Cammi, R.; Mennucci, B.; Pomelli, C.; Adamo, C.; Clifford, S.; Ochterski, J.; Petersson, G. A.; Ayala, P. Y.; Cui, Q.; Morokuma, K.; Malick, D. K.; Rabuck, A. D.; Raghavachari, K.; Foresman, J. B.; Cioslowski, J.; Ortiz, J. V.; Stefanov, B. B.; Liu, G.; Liashenko, A.; Piskorz, P.; Komaromi, I.; Gomperts, R.; Martin, R. L.; Fox, D. J.; Keith, T.; Al-Laham, M. A.; Peng, C. Y.; Nanayakkara, A.; Gonzalez, C.; Challacombe, M.; Gill, P. M. W.; Johnson, B. G.; Chen, W.; Wong, M. W.; Andres, J. L.; Head-Gordon, M.; Replogle, E. S.; Pople, J. A. *Gaussian 98*, revision A.9; Gaussian, Inc.: Pittsburgh, PA, 1998.
- (50) Noury, S.; Krokidis, X.; Fuster, F.; Silvi, B. Topmod package, 1997.
- (51) Hiberty, P. C.; Himbel, S.; Danovich, D.; Shaik, S. *J. Am. Chem. Soc.* **1995**, *117*, 9003.
- (52) Tureček, F. *Collect. Czech. Chem. Commun.* **2000**, *65*, 455.
- (53) Janousek, B. K.; Brauman, J. *Phys. Rev. A* **1980**, *23*, 1673.
- (54) Smith, J.; Kim, J.; Lineberger, W. *Phys. Rev. A* **1997**, *55*, 2036.
- (55) Schwartz, R.; Davico, G.; Lineberger, W. *J. Electron Spectrosc. Relat. Phenom.* **2000**, *108*, 163.
- (56) Snow, K.; Thomas, T. *Int. J. Mass Spectrom. Ion Processes* **1990**, *96*, 49.
- (57) Walters, E.; Blais, N. *J. Chem. Phys.* **1984**, *80*, 3501.
- (58) Nourbakhsh, S.; Norwood, K.; Yin, H.-M.; Liao, C.-L.; Ng, C. Y. *J. Chem. Phys.* **1991**, *95*, 946.
- (59) Akopyan, M.; Sergeev, Y.; Vilesov, F. *High Energy Chem.* **1970**, *4*, 265, In original 305.